Some Properties of Nonlinear Wave Systems

By J. Yang and D. J. Benney

The results of a preliminary study of a particular nonlinear system of partial differential equations are presented. While much of this work pertains to two coupled nonlinear Schrödinger equations, it is believed that the properties found are representative of many other dispersive wave systems.

1. Introduction

Nonlinear wave phenomena remain poorly understood, and significant results are limited to either very special examples or situations for which perturbation methods are adequate. The former case is typified by exactly solvable equations and the important role played by solitons. For the latter class of problems, the evolution of weak interactions, resonances, and slowly varying wave trains are well-known examples. Despite the limitations of each approach, these studies have stimulated a large volume of mathematical research and considerable interest in the applied disciplines.

One objective of the present paper is to report on some results for nonlinear wave systems that do not fall into either of the above categories. The approach taken is to study a particular case in some detail and, on the basis of the results obtained, to speculate on some anticipated general characteristics of nonlinear

Address for correspondence: Dr. D. J. Benney, Room 2-341, Massachusetts Institute of Technology, 77 Massachusetts Avenue, Cambridge, MA 02139-4307

STUDIES IN APPLIED MATHEMATICS 96:111–139

Published by Blackwell Publishers, 238 Main Street, Cambridge, MA 02142, USA, and 108 Cowley Road, Oxford, OX4 1JF, UK.

dispersive wave systems. It is in this vein that some tentative general ideas are proposed.

The case of two coupled Schrödinger equations is taken to be a typical problem. Such equations arise in a great variety of wave phenomena. In particular, for surface waves a strong interaction between wave packets exists if certain rather mild geometrical constraints are satisfied [1, 2]. Special values of the coupling constants are of interest in nonlinear optics [3, 4]. Internal waves are another application of potential importance.

In one spatial dimension, the set of equations of interest is

$$iA_t = A_{xx} + (AA^* + \beta BB^*)A, \tag{1.1}$$

$$iB_t = B_{xx} + (\beta AA^* + BB^*)B, \tag{1.2}$$

with $A(x, 0)$, $B(x, 0)$, and the value of the real constant β prescribed. It is desirable to understand the evolution of the two wave envelope functions A and B. The emphasis here is on the word *understand* because our analysis does not predict quantitative evolution of the functions A and B, but only the qualitative features to be expected. To this end, numerical and analytical methods will be used to reinforce each other whenever possible.

The particular choice of (1.1) and (1.2) with just one parameter β is governed by several factors. Firstly, if $\beta = 0$, the equations decouple and each equation is solvable with potential soliton structure. If $\beta = 1$, the system (1.1) and (1.2) has been shown to be solvable by the inverse scattering method (see Manakov [5]). For other values of β, the system is not exactly solvable and interactions between solitary waves are generally nonelastic. It will be seen that the value of the parameter β plays an important role in determining the nature of the long-time solutions.

For nonlinear Schrödinger systems, the mixed state describing uniform periodic finite amplitude waves may be stable or unstable. In its simplest form, this instability mechanism was verified both theoretically and experimentally in water waves by Benjamin and Feir [6], and in more complicated situations by Roskes [2]. Here the standard linear stability analysis is not reproduced.

2. Solitary wave solutions

It will become apparent that the permanent wave solutions provide the key to understanding the long-time behavior of the system (1.1) and (1.2). With this in mind, consider solutions to (1.1) and (1.2) of the form

$$A = e^{-i(U/2)x - i(\omega_1 - (U^2/4))t} r_1(x - Ut), \tag{2.1}$$

$$B = e^{-i(U/2)x - i(\omega_2 - (U^2/4))t} r_2(x - Ut), \tag{2.2}$$

in which case r_1 and r_2 satisfy the equations

$$r_{1\xi\xi} - \omega_1 r_1 + (r_1^2 + \beta r_2^2) r_1 = 0, \tag{2.3}$$

$$r_{2\xi\xi} - \omega_2 r_2 + (r_2^2 + \beta r_1^2) r_2 = 0, \tag{2.4}$$

where $\xi = x - Ut$. For solitary waves with exponential decay as $|\xi| \to \infty$, it is necessary that $\omega_1, \omega_2 > 0$. A change of scale ensures that $\omega_1 = 1$ without any loss of generality. Note that if r_1 (or r_2) is a solution, then so is $-r_1$ (or $-r_2$).

The system (2.3) and (2.4) is a nonlinear eigenvalue system, and the solution structures are complicated. If r_1 is zero, then

$$r_2 = \sqrt{2\omega_2}\,\operatorname{sech}\sqrt{\omega_2}\xi \tag{2.5}$$

and the solution is degenerate. However, for any given values of β, ω_1 (> 0), and ω_2 (> 0), the system has an infinite number of nondegenerate solutions. In special cases, these solutions can be found analytically, but numerical methods provide a more effective alternative. Some typical results are shown in Figures 1, 2, 3, 4, and 5 with the values for β of 3, 2, 1, 2/3, and $-2/3$, respectively. In these figures, ω_1 is scaled to be equal to unity. The solid curves are r_1 plots, and the dashed ones are r_2 plots.

One special solution is the equally mixed solitary-wave solution. This corresponds to the case with $\omega_1 = \omega_2 = 1$,

$$r_1(\xi) = r_2(\xi) = \sqrt{\frac{2}{1+\beta}}\,\operatorname{sech}\xi, \tag{2.6}$$

provided $\beta > -1$. Figures 1a, 2a, 3a, 4a, and 5a belong to this class of solutions.

Another important category corresponds to the so-called wave and daughter wave solutions. These arise if for any value of β the solutions are such that $r_2 \ll r_1$ (or $r_1 \ll r_2$), in which case r_2 (or r_1) is called a daughter wave. Not unexpectedly, these solutions can be found by asymptotic methods.

For example, if $r_2 \ll r_1$ and ω_1 is scaled to be equal to unity, the leading-order terms in (2.3) and (2.4) give

$$r_{1\xi\xi} - r_1 + r_1^3 = 0, \tag{2.7}$$

$$r_{2\xi\xi} - \omega_2 r_2 + \beta r_1^2 r_2 = 0. \tag{2.8}$$

Equation (2.7) yields

$$r_1 = \sqrt{2}\,\operatorname{sech}\xi \tag{2.9}$$

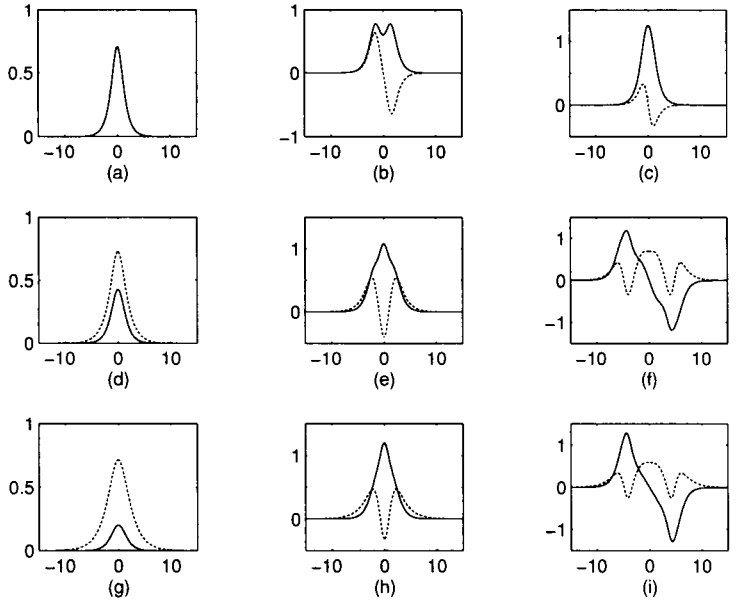

Figure 1. Solutions $r_1(\xi)$ and $r_2(\xi)$ of equations (2.3) and (2.4) with $\beta = 3$. In (**a**), (**b**), and (**c**), $\omega_2 = 1$; in (**d**), (**e**), and (**f**), $\omega_2 = 0.5$; in (**g**), (**h**), and (**i**), $\omega_2 = 0.3$.

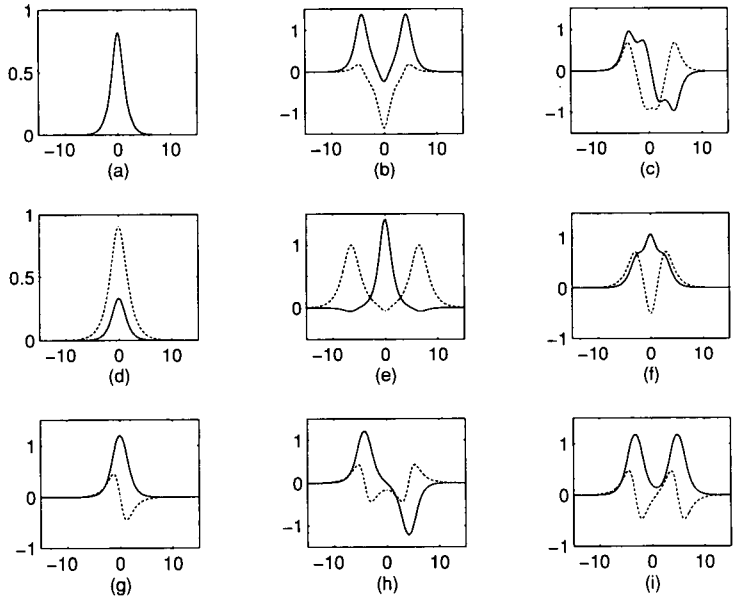

Figure 2. Solutions $r_1(\xi)$ and $r_2(\xi)$ of equations (2.3) and (2.4) with $\beta = 2$. In (**a**), (**b**), and (**c**), $\omega_2 = 1$; in (**d**), (**e**), (**f**), (**g**), (**h**), and (**i**), $\omega_2 = 0.5$.

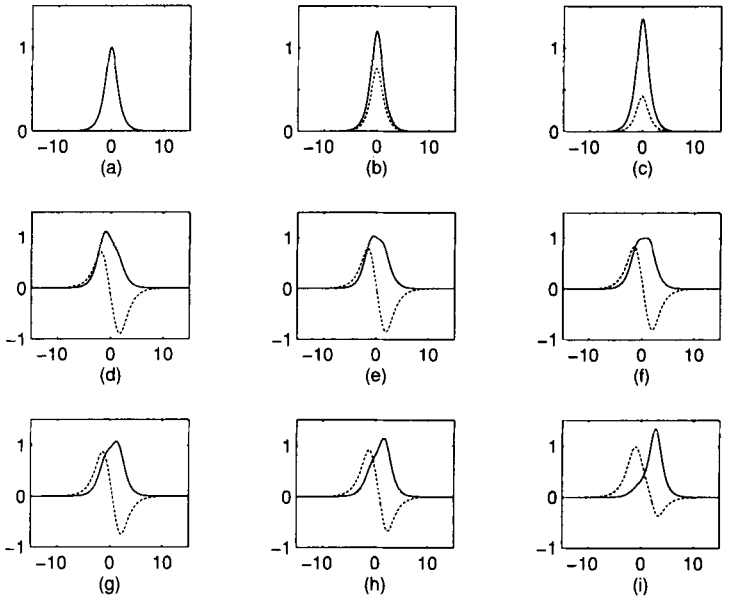

Figure 3. Solutions $r_1(\xi)$ and $r_2(\xi)$ of equations (2.3) and (2.4) with $\beta = 1$. In (**a**), (**b**), and (**c**), $\omega_2 = 1$; in (**d**), (**e**), (**f**), (**g**), (**h**), and (**i**), $\omega_2 = 0.5$.

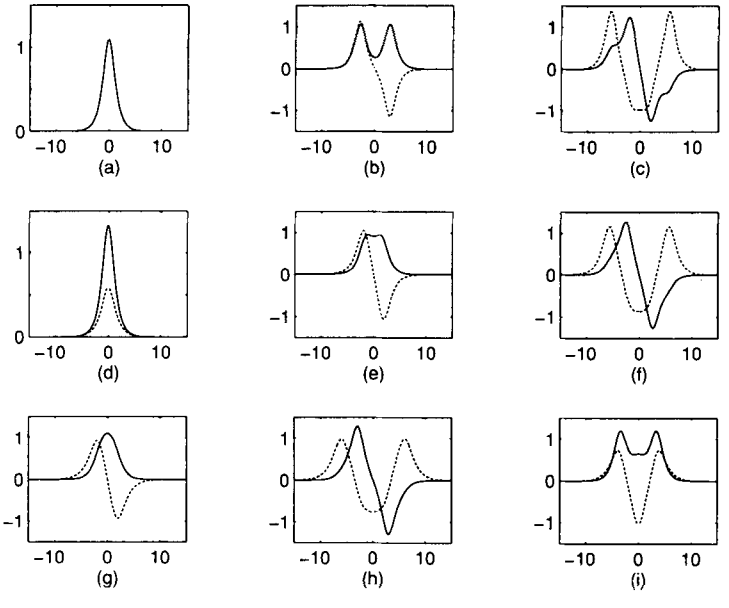

Figure 4. Solutions $r_1(\xi)$ and $r_2(\xi)$ of equations (2.3) and (2.4) with $\beta = 2/3$. In (**a**), (**b**), and (**c**), $\omega_2 = 1$; in (**d**), (**e**), and (**f**), $\omega_2 = 0.7$; in (**g**), (**h**), and (**i**), $\omega_2 = 0.5$.

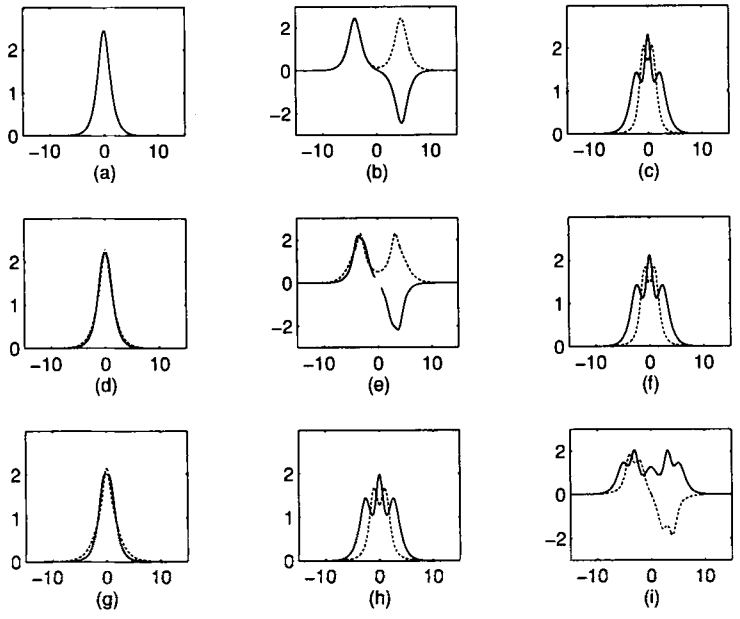

Figure 5. Solutions $r_1(\xi)$ and $r_2(\xi)$ of equations (2.3) and (2.4) with $\beta = -2/3$. In (**a**), (**b**), and (**c**), $\omega_2 = 1$; in (**d**), (**e**), and (**f**), $\omega_2 = 0.7$; in (**g**), (**h**), and (**i**), $\omega_2 = 0.5$.

so that (2.8) becomes

$$r_{2\xi\xi} - \omega_2 r_2 + 2\beta \operatorname{sech}^2 \xi r_2 = 0. \tag{2.10}$$

Solutions to (2.10) that have the property that $r_2 \to 0$ as $|\xi| \to \infty$ are well known. The equation can be transformed into a hypergeometric equation (see Landau & Lifshitz [7]), and the eigenvalue relation is given by

$$\omega_2 = \frac{1}{4}[\sqrt{1 + 8\beta} - (1 + 2n)]^2, \tag{2.11}$$

where n is a non-negative integer. There are a finite number of eigenvalues, because it is necessary that $n < (\sqrt{1 + 8\beta} - 1)/2$. More daughter waves are possible as β increases, as indicated below.

1. $\beta < 0$. No value of n is possible, and no daughter waves exist.
2. $0 < \beta \leq 1$, $n = 0$, and $\omega_2 = [\sqrt{1 + 8\beta} - 1]^2/4$. There is only one daughter wave, with

$$r_2 = \operatorname{sech}^s \xi, \qquad s = \frac{1}{2}(\sqrt{1 + 8\beta} - 1). \tag{2.12}$$

This solution is even in ξ.

3. $1 < \beta \leq 3$, $n = 0$ or 1. There are two daughter wave modes, namely,

$$r_2 = \operatorname{sech}^s \xi, \quad \text{and} \quad r_2 = \operatorname{sech}^s \xi \sinh \xi, \tag{2.13}$$

with $s = (\sqrt{1 + 8\beta} - 1)/2$. The first daughter wave is even and the second is odd.

The solutions r_1, r_2, and ω_2 obtained above are the leading-order solutions for the wave–daughter wave structures. Higher-order terms can be found by standard perturbation methods, but the details will not be presented here. Note that Figures 1c,g, 2d,g, 3c, and 4d are essentially wave–daughter wave configurations.

In the special case $\beta = 3$, $\omega_1 = \omega_2 = 1$, the pair of equations (2.3) and (2.4) decouple, and both $r_1 + r_2$ and $r_1 - r_2$ satisfy the equation

$$r_{\xi\xi} - r + r^3 = 0, \tag{2.14}$$

so that a particular solution set is given by

$$r_1 = \frac{\sqrt{2}}{2}[\operatorname{sech}(\xi - \xi_0) + \operatorname{sech}(\xi + \xi_0)], \tag{2.15}$$

$$r_2 = \frac{\sqrt{2}}{2}[\operatorname{sech}(\xi - \xi_0) - \operatorname{sech}(\xi + \xi_0)]. \tag{2.16}$$

Figure 1b,c belongs to this class of solutions. Note that when $\xi_0 \to 0$,

$$r_1 \approx \sqrt{2} \operatorname{sech} \xi, \qquad r_2 \approx \sqrt{2}\xi_0 \operatorname{sech} \xi \tanh \xi, \tag{2.17}$$

and the solution reduces to a wave–daughter wave configuration.

Finally, another special case should be mentioned. This occurs when $\beta = 1$, $\omega_1 = \omega_2 = 1$, in which case

$$r_1 = \sqrt{2} \cos \alpha \operatorname{sech} \xi, \qquad r_2 = \sqrt{2} \sin \alpha \operatorname{sech} \xi \tag{2.18}$$

is a solution. Figure 3a,b,c belongs to this class of solutions. Clearly, for limiting values of α it is possible to return to the wave–daughter wave solution.

3. Linear stability of permanent waves

The solitary wave solutions identified in the previous section are of importance because they provide the dominant behavior of the long-time solution to the initial-value problem. For this reason, it is critical to know which of these solutions are stable (at least within the framework of linear theory), because these

are the only ones that will survive. In this section, a few special cases are studied analytically and numerical evidence for more general configurations is presented.

Firstly, note that the degenerate solutions (see equation (2.5)) are known to be stable (Zakharov and Shabat [8]). Next, consider the equally mixed solitary waves as given by

$$A = B = e^{-i(U/2)x - i(1-(U^2/4))t} \sqrt{\frac{2}{1+\beta}} \operatorname{sech}(x - Ut). \tag{3.1}$$

A temporary change of notation is convenient in that with

$$\bar{x} = x - Ut, \qquad \bar{t} = t, \tag{3.2}$$

$$\begin{pmatrix} A \\ B \end{pmatrix} = e^{-i(U/2)x + i(U^2/4)t} \begin{pmatrix} \bar{A} \\ \bar{B} \end{pmatrix}. \tag{3.3}$$

The stability analysis proceeds by writing

$$\bar{A} = e^{-i\bar{t}} \left\{ \sqrt{\frac{2}{1+\beta}} \operatorname{sech} \bar{x} + A' \right\}, \tag{3.4}$$

$$\bar{B} = e^{-i\bar{t}} \left\{ \sqrt{\frac{2}{1+\beta}} \operatorname{sech} \bar{x} + B' \right\} \tag{3.5}$$

and linearizing in the primed variables. With the bars and primes discarded, the equations of interest are

$$iA_t = A_{xx} - A + \frac{\operatorname{sech}^2 x}{1+\beta} \{2(2+\beta)A + 2A^* + 2\beta(B + B^*)\}, \tag{3.6}$$

$$iB_t = B_{xx} - B + \frac{\operatorname{sech}^2 x}{1+\beta} \{2(2+\beta)B + 2B^* + 2\beta(A + A^*)\}. \tag{3.7}$$

Again, the couplings involved are clarified if the real variables p, q, r, and s are introduced, where

$$A + B = p + iq, \qquad A - B = r + is, \tag{3.8}$$

in which case the following set of equations arises:

$$-\frac{\partial p}{\partial t} + \left(\frac{\partial^2}{\partial x^2} - 1 + 2\operatorname{sech}^2 x \right) q = 0, \tag{3.9}$$

$$\frac{\partial q}{\partial t} + \left(\frac{\partial^2}{\partial x^2} - 1 + 6\,\mathrm{sech}^2 x\right) p = 0, \tag{3.10}$$

$$-\frac{\partial r}{\partial t} + \left(\frac{\partial^2}{\partial x^2} - 1 + 2\,\mathrm{sech}^2 x\right) s = 0, \tag{3.11}$$

$$\frac{\partial s}{\partial t} + \left(\frac{\partial^2}{\partial x^2} - 1 + \frac{2(3-\beta)}{1+\beta}\,\mathrm{sech}^2 x\right) r = 0. \tag{3.12}$$

This eighth-order system decouples into two independent fourth-order systems. If $e^{\lambda t}$ solutions are sought, the (p, q) system is independent of β and has stable solutions $\lambda = 0$, $p = \mathrm{sech}\, x$, $q = \mathrm{sech}\, x \tanh x$. The more interesting (r, s) system depends on β and is less simple to analyze. (Note that these latter solutions correspond to motions such that $A = -B$.) Perturbation methods are effective for β small, and the limiting eigenvalues λ will be of interest. The equations

$$\left(\frac{d^2}{dx^2} - 1 + \frac{2(3-\beta)}{1+\beta}\,\mathrm{sech}^2 x\right) r + \lambda s = 0, \tag{3.13}$$

$$\left(\frac{d^2}{dx^2} - 1 + 2\,\mathrm{sech}^2 x\right) s - \lambda r = 0 \tag{3.14}$$

are to be solved with $r, s \to 0$ as $|x| \to \infty$. With $\beta = \lambda = 0$, there is a solution $r = \mathrm{sech}\, x \tanh x$, $s = \mathrm{sech}\, x$ so that perturbation solutions are sought of the form

$$r = r^{(0)} + \gamma r^{(1)} + \cdots, \tag{3.15}$$

$$s = s^{(0)} + \gamma s^{(1)} + \cdots, \tag{3.16}$$

$$\lambda = \qquad \gamma \lambda^{(1)} + \cdots, \tag{3.17}$$

where $\beta = \delta\gamma^2$, $\gamma > 0$, and $\delta = \pm 1$. Standard methods yield, to leading order, the result

$$\lambda^2 = -\frac{64}{15}\beta. \tag{3.18}$$

To this level of approximation, the equally mixed solitary wave solution is stable for β small and positive ($\delta = +1$) and unstable for β small and negative ($\delta = -1$).

When $\beta < 0$ but not small, numerical results show that there is still instability. One such example is shown in Figure 16. For $\beta > 0$, numerical experiments show that the equally mixed solitary wave solution remains stable. Consequently, the solutions in Figures 1a, 2a, 3a, and 4a are stable, whereas the solution shown in Figure 5a is unstable.

If we return to the special case $\beta = 3$ considered in Section 2 (see equation (2.15) and (2.16)), it is possible to determine the stability by analytical methods.

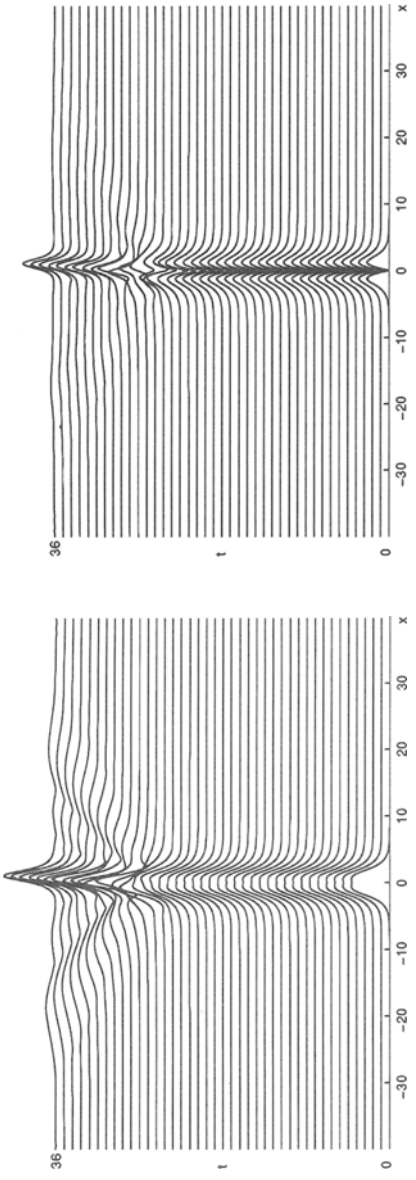

Figure 6. Instability and time evolution of the class of special solutions (2.1), (2.2), (2.15), and (2.16) for $\beta = 3$ when $\xi_0 \neq 0$. In this particular case, ξ_0 is taken to be 1. The left figure is the $|A(x,t)|$ evolution, and the right figure is the $|B(x,t)|$ evolution.

However, only the numerical experiments are reported here. It is found that the solutions (2.15) and (2.16) are always unstable for all $\xi_0 \neq 0$. A typical case is shown in Figure 6. In view of this result, the solutions in Figure 1b,c are unstable.

In another special case with $\beta = 1$, it was pointed out earlier that the equations (1.1) and (1.2) are solvable by inverse scattering methods. The permanent wave solutions with $\omega_1 = \omega_2$ are solitons and are certainly stable. Examples are shown in Figure 3a,b,c. Other permanent wave solutions of the form (2.1) and (2.2) with $\omega_1 \neq \omega_2$ are unstable. A few solutions of this type are given in Figure 3d,e,f,g,h,i.

Finally, some comments on the stability of general permanent wave solutions (2.1) and (2.2) are warranted. This is a more difficult question, but much insight can be gained in view of the earlier results. In the following paragraph, we speculate (based on numerics) on the stability properties.

For $\beta > 0$, the degenerate solutions are stable. The equally mixed solutions (3.1), as shown in Figures 1a, 2a, 3a, and 4a, are stable. The special solutions (2.18) for $\beta = 1$, as shown in Figure 3a,b,c, are also stable. These stable solutions are such that both r_1 and r_2 are centered together and have only one extremum. There is evidence that other such solutions, as in Figure 1d,g, 2d, and 4d, are also stable. On the other hand, the special solutions (2.15), (2.16) for $\beta = 3$ (as shown in Figure 1b,c), and the special solutions for $\beta = 1$ with $\omega_1 \neq \omega_2$ (as shown in Figure 3d,e,f,g,h,i), are unstable. These unstable solutions are such that at least one of r_1 and r_2 has more than one extremum. So there is some reason to believe that other such solutions, as in Figure 1e,f,h,i, 2b,c,e,f,g,h,i, 4b,c,e,f,g,h,i, are also unstable. Actually, complicated solutions, as in Figure 1f,i, etc., are almost certainly unstable.

For $\beta > 0$, a reasonable rule of thumb would appear to be that the permanent wave solutions (2.1) and (2.2) are stable if and only if both r_1 and r_2 are centered together and have only one extremum. For $\beta < 0$, even those solutions appear to be unstable unless they are degenerate. One piece of evidence is the fact that the equally mixed solutions (3.1) are unstable when $\beta < 0$.

It should be noted that when β is positive and is not equal to 1, nondegenerate stable solutions r_1 and r_2 exist for a certain range of values of ω_2/ω_1. This range is dependent on the value of β and is easy to determine. Once ω_1 and ω_2 are specified, these stable solutions are also unique. When β is equal to 1, the nondegenerate stable solutions r_1 and r_2 exist for equal values of ω_1 and ω_2 and are not unique if $\omega_1 (= \omega_2)$ is given (see equation (2.18)). In both cases, nondegenerate stable solutions are abundant.

4. Solitary wave interactions

In this section, the interaction of two solitary waves is studied. The initial values taken are

$$A(x, 0) = \sqrt{2}\, r_{A0} \operatorname{sech} r_{A0}(x - x_{A0}) e^{-i(U_{A0}/2)x}, \tag{4.1}$$

$$B(x, 0) = \sqrt{2}\, r_{B0} \operatorname{sech} r_{B0}(x - x_{B0}) e^{-i(U_{B0}/2)x} \tag{4.2}$$

Initially, A is a solitary wave centered at $x = x_{A0}$ with speed U_{A0} and amplitude $\sqrt{2}r_{A0}$, and B is another solitary wave centered at $x = x_{B0}$ with speed U_{B0} and amplitude $\sqrt{2}r_{B0}$. The interaction between these two solitary waves is generally nonelastic. A numerical study of this type of interaction was first made for various values of β and different initial conditions of the form (4.1) and (4.2). Some results are shown in Figures 7–12. In these figures, the left and right halves are the $|A(x, t)|$ and $|B(x, t)|$ plots, respectively.

The interaction in Figure 7 is typical for initially well-separated solitary waves (4.1) and (4.2) when $\beta > 0$ and not very large. After the interaction, the two waves pass through each other with some reshaping and radiation shedding, and daughter waves are generated. These daughter waves are small pulses that split off from a solitary wave and propagate along beside it but in the other mode. It should be recalled that these waves are exactly those special permanent wave solutions discussed in Section 2, where their shapes were determined asymptotically. The amplitudes of the daughter waves and the amount of radiation are dependent on the initial conditions and the value of β, but the qualitative structures remain the same (see Figure 8). When $\beta < 0$, if the approach velocity $U_{A0} - U_{B0}$ is not large, then the two initially well-separated solitary waves (4.1) and (4.2) are always reflected off each other after the interaction, as shown in Figure 9. There is also some radiation, but the amount is very small. If the approach velocity $U_{A0} - U_{B0}$ is large, then these two solitary waves break up after the interaction, as shown in Figure 10. For each wave, part of the energy is transmitted and part is reflected. If the approach velocity is very large, then these two waves will pass through each other. If initially the two solitary waves overlap, the interaction scenario is quite different. For $\beta > 0$, they tend to trap each other and form a bound, oscillatory state as shown in Figure 11. For $\beta < 0$, they escape from each other as shown in Figure 12.

In order to have some understanding of these results, it is instructive to consider the motion of a solitary wave in a slowly varying potential field. This motion is governed by the equation

$$iA_t = A_{xx} + (AA^* - f(X))A, \tag{4.3}$$

where $X = \epsilon x$ ($\epsilon \ll 1$) and $f(X)$ is a given slowly varying function. The initial value is

$$A(x, 0) = \sqrt{2}r \operatorname{sech} r\, x e^{-i(U/2)x} \tag{4.4}$$

and corresponds to a solitary wave of speed U and amplitude $\sqrt{2}r$. Due to the slowly varying potential field, this wave will undergo slow changes. A multiple-scale perturbation analysis provides a simple way to determine this evolution.

The appropriate form of solution A is

$$A = e^{i\{r^2 - (U^2/4) - f(X)\}(\theta - \theta_0) - i(\sigma - \sigma_0)} q(\theta, X, \epsilon), \tag{4.5}$$

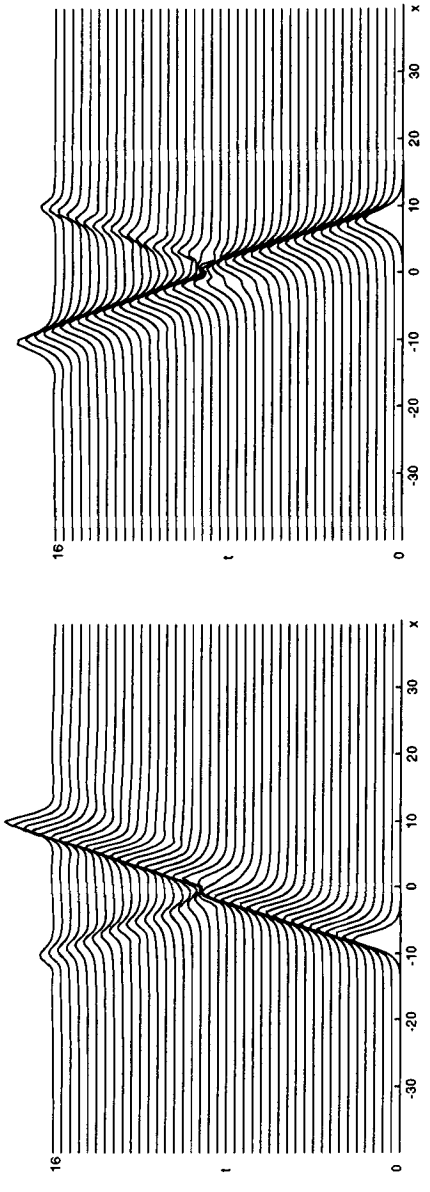

Figure 7. The interaction of two initially well-separated solitary waves for $\beta = 2$. The initial condition is given by (4.1) and (4.2) with $r_{A0} = 1, U_{A0} = 1, x_{A0} = -8; r_{B0} = 0.8, U_{B0} = -1, x_{B0} = 8; 0 \leq t \leq 16$. Note that the two waves pass through each other after the interaction, and small daughter waves are generated.

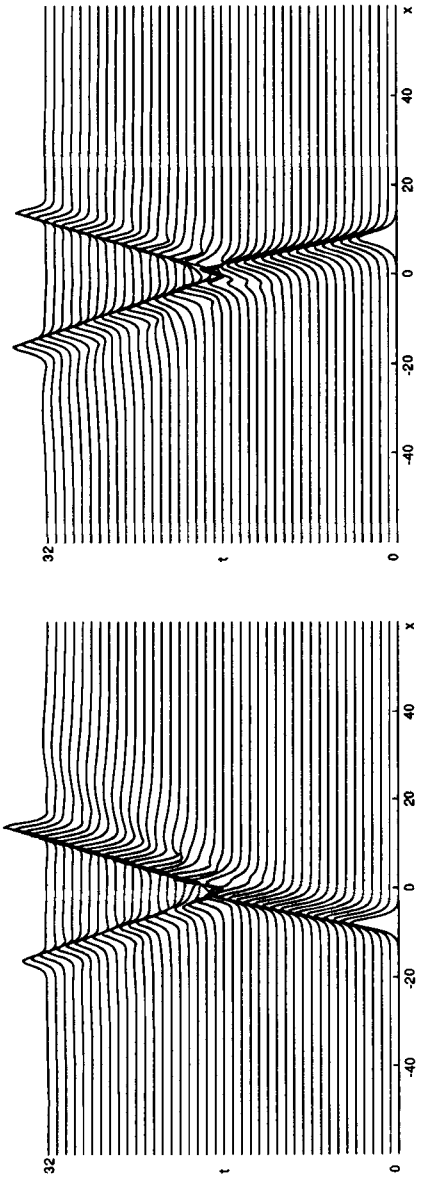

Figure 8. The interaction of two initially well-separated solitary waves for $\beta = 2$. The initial condition is the same as in Figure 7 except that here $U_{A0} = 0.5$ and $U_{B0} = -0.5$; $0 \leq t \leq 32$. Note that the daughter waves become larger when the approach velocity $U_{A0} - U_{B0}$ of the two waves gets smaller.

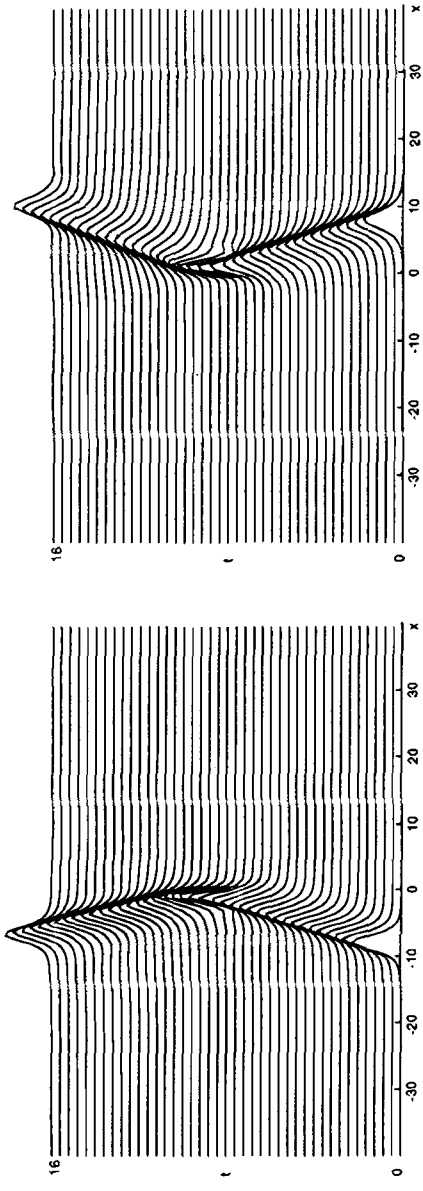

Figure 9. The interaction of two initially well-separated solitary waves for $\beta = -2$. The initial condition is the same as in Figure 7; $0 \leq t \leq 16$. Note that the two solitary waves are reflected off each other after the interaction.

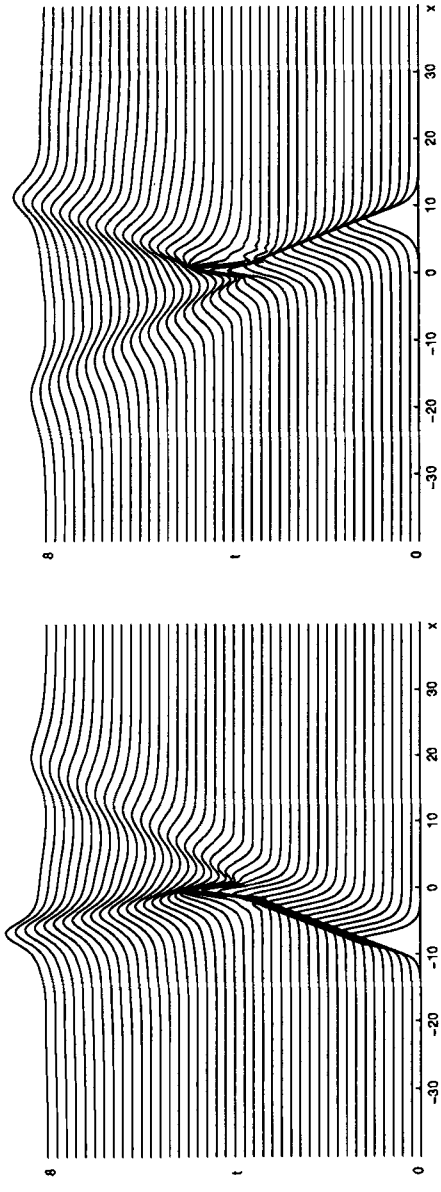

Figure 10. The interaction of two initially well-separated solitary waves for $\beta = -2$. The initial condition is the same as in Figure 7 except that here $U_{A0} = 2.7$ and $U_{B0} = -2.7$; $0 \leq t \leq 8$. Note that the two solitary waves break up after the interaction.

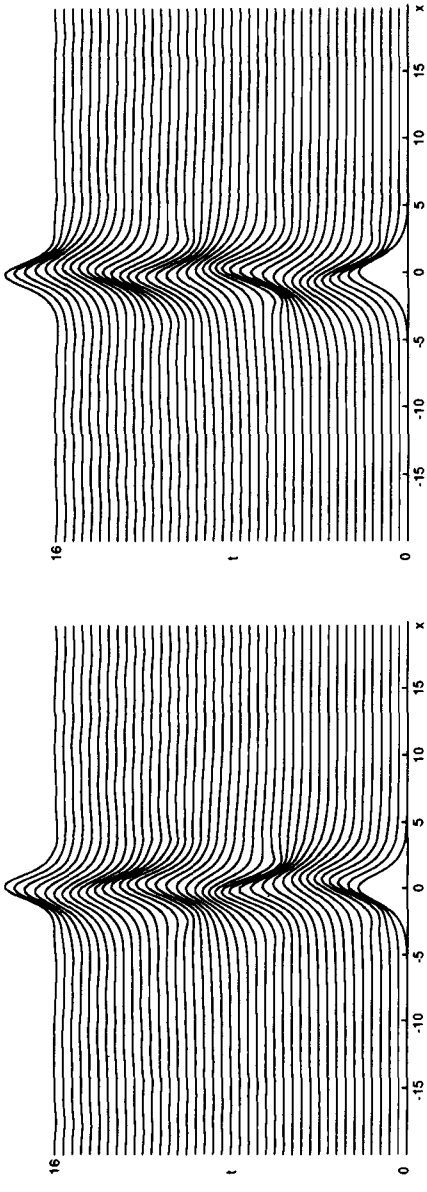

Figure 11. The interaction of two initially overlapping solitary waves for $\beta = 0.2$. The initial condition is given by (4.1) and (4.2) with $r_{A0} = 1, U_{A0} = 0.6, x_{A0} = 0; r_{B0} = 1, U_{B0} = -0.6, x_{B0} = 0; 0 \leq t \leq 16$. These two solitary waves are trapped by each other and undergo an oscillating motion.

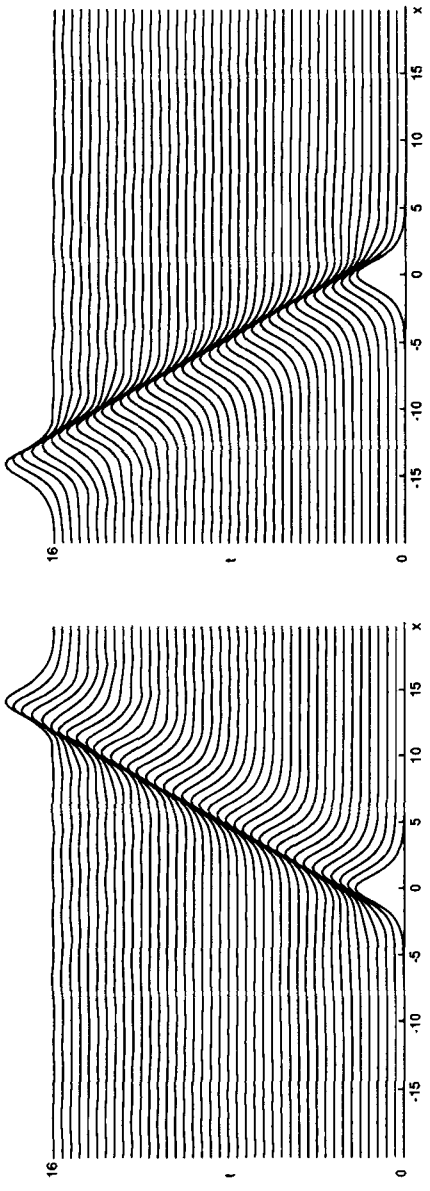

Figure 12. The interaction of two initially overlapping solitary waves for $\beta = -0.2$. The initial condition is the same as in Figure 11; $0 \leq t \leq 16$. These two solitary waves escape from each other.

where

$$\frac{\partial\theta}{\partial x} = \frac{1}{U}, \qquad \frac{\partial\theta}{\partial t} = -1, \tag{4.6}$$

and

$$\frac{\partial\sigma}{\partial x} = \frac{1}{U}\left\{r^2 + \frac{U^2}{4} - f(X)\right\}, \qquad \frac{\partial\sigma}{\partial t} = 0. \tag{4.7}$$

Here, U, r, θ_0, and σ_0 are functions of the slow space variable X.

The substitution of (4.5) into (4.3) yields

$$\frac{q_{\theta\theta}}{U^2} - r^2 q + q^2 q^* = \epsilon F(q), \tag{4.8}$$

where

$$\begin{aligned} F(q) = &-\left\{U\left[r^2 - \frac{U^2}{4} - f(X)\right]_X (\theta - \theta_0)q + \frac{2q_{\theta X}}{U} + \left(\frac{1}{U}\right)_X q_\theta \right. \\ &\left. - U\left[r^2 - \frac{U^2}{4} - f(X)\right]\theta_{0X} q + U\sigma_{0X} q\right\} \\ &-i\left\{\frac{1}{U}\left[r^2 - \frac{U^2}{4} - f(X)\right]_X [q + 2(\theta - \theta_0)q_\theta] - \frac{U_X}{2}q - Uq_X \right. \\ &\left. - \frac{2[r^2 - \frac{U^2}{4} - f(X)]}{U}\theta_{0X} q_\theta + \frac{2}{U}\sigma_{0X} q_\theta\right\}. \end{aligned} \tag{4.9}$$

The function $q(\theta, X, \epsilon)$ is expanded in the form

$$q(\theta, X, \epsilon) = q_0(\theta, X) + \epsilon q_1(\theta, X) + \cdots, \tag{4.10}$$

where

$$q_0 = \sqrt{2}r \operatorname{sech} rU(\theta - \theta_0) \tag{4.11}$$

is the leading-order term.

At order ϵ, from (4.8) and (4.9) it is found that

$$\frac{1}{U^2}q_{1\theta\theta} - r^2 q_1 + 2q_0^2 q_1 + q_0^2 q_1^* = F_1, \tag{4.12}$$

where $F_1 = F(q_0)$. Upon writing $q_1 = \phi_1 + i\psi_1$, where ϕ_1 and ψ_1 are real-valued functions, the above equation becomes

$$L\phi_1 \equiv \frac{1}{U^2}\phi_{1\theta\theta} - r^2\phi_1 + 3q_0^2\phi_1 = \operatorname{Re} F_1, \tag{4.13}$$

$$M\psi_1 \equiv \frac{1}{U^2}\psi_{1\theta\theta} - r^2\psi_1 + q_0^2\psi_1 = \operatorname{Im} F_1. \tag{4.14}$$

Note that the operators L and M are self-adjoint and $Lq_{0\theta} = 0$, $Mq_0 = 0$. For equations (4.13) and (4.14) to have localized solutions ϕ_1 and ψ_1 around the solitary wave, the solvability conditions

$$\int_{-\infty}^{\infty} q_{0\theta} \operatorname{Re} F_1 \, d\theta = 0, \tag{4.15}$$

$$\int_{-\infty}^{\infty} q_0 \operatorname{Im} F_1 \, d\theta = 0 \tag{4.16}$$

have to be satisfied. From (4.15) and (4.16), the evolution equations for r and U are found to be

$$\frac{dr}{dX} = 0, \qquad \frac{d(f(X) + \frac{U^2}{4})}{dX} = 0 \tag{4.17}$$

so that to the leading-order approximation

$$r = \text{constant}, \tag{4.18}$$

$$f(X) + \frac{U^2}{4} = \text{constant}. \tag{4.19}$$

The relations (4.18) and (4.19) are asymptotically accurate for $\epsilon \ll 1$. Numerical results show that they are quite good even for ϵ close to unity.

With (4.18) and (4.19), the solutions ϕ_1 and ψ_1 can be easily determined from (4.13) and (4.14). The slow evolution equations for the position shift θ_0 and the phase shift σ_0 are obtained by imposing the orthogonality conditions

$$\int_{-\infty}^{\infty} q_0\phi_1 \, d\theta = 0, \qquad \int_{-\infty}^{\infty} q_{0\theta}\psi_1 \, d\theta = 0, \tag{4.20}$$

but the details will not be pursued here.

An alternative derivation of the relations (4.18) and (4.19) can be given by using the conservation laws. From equation (4.3), the following three conservation relations are found:

1. Mass conservation,

$$\int_{-\infty}^{\infty} |A|^2 \, dx = \text{constant}. \tag{4.21}$$

2. Momentum conservation,

$$i\frac{d}{dt}\int_{-\infty}^{\infty} (AA_x^* - A^*A_x) \, dx = 2\int_{-\infty}^{\infty} |A|^2 f_x \, dx. \tag{4.22}$$

3. Energy conservation,

$$\int_{-\infty}^{\infty} \left(|A_x|^2 - \frac{1}{2}|A|^4 + f(X)|A|^2 \right) dx = \text{constant}. \tag{4.23}$$

Locally, a solitary wave with speed U and amplitude $\sqrt{2}r$ is of the form

$$A = \sqrt{2}r \operatorname{sech} r(x - x_0 - Ut) e^{-i(U/2)(x-Ut) - i(r^2 + (U^2/4))t + if(X)t - i\theta_0}. \tag{4.24}$$

Because the potential field varies slowly, it is reasonable to assume that this form almost remains the same. Making use of equation (4.24), it is found that

$$\int_{-\infty}^{\infty} |A|^2 \, dx = 4r, \tag{4.25}$$

$$\int_{-\infty}^{\infty} \left(|A_x|^2 - \frac{1}{2}|A|^4 + f(X)|A|^2 \right) dx \approx 4r \left(\frac{U^2}{4} + f(X) - \frac{1}{3}r^2 \right), \tag{4.26}$$

where X in the right-hand side of equation (4.26) is implied to be the center position of the solitary wave. The mass and energy conservation (4.21) and (4.23) readily recover the relations (4.18) and (4.19).

It should be noted that the momentum conservation relation (4.22) is automatically satisfied by (4.18) and (4.19).

The approximate relations (4.18) and (4.19) offer much insight into the motion of a solitary wave in a slowly varying potential field. The relation (4.18) indicates that the amplitude of the solitary wave does not change as it travels through the potential field. The relation (4.19) shows that the speed of the wave will change as $f(X)$ varies. When $f(X)$ decreases, the wave will accelerate; when $f(X)$ increases, the wave will slow down. In the latter case, if $f(X)$ gets large enough, the solitary wave will lose all its speed and come to a stop. It can be shown that this wave cannot stay there because such a state is unstable. What the wave does is reverse direction, i.e., it is reflected by the potential field. This is very much like the motion of a particle in a potential well. The condition for reflection is

$$\frac{U_0^2}{4} + f(X_0) < \max(f(X)), \tag{4.27}$$

where U_0 is the initial wave velocity and X_0 is the initial center position of the wave. All these theoretical predictions agree very well with our numerical calculations from equation (4.3) for both small and moderate values of ϵ. Two such numerical calculations are shown in Figure 13 and 14. In both cases, initially the solitary wave is

$$A(x, 0) = \sqrt{2} \operatorname{sech}(x + 24) e^{-(i/2)(x+24)}, \tag{4.28}$$

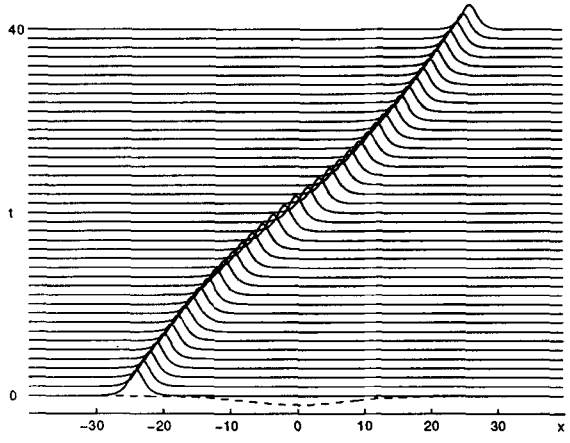

Figure 13. Passing through of a solitary wave in a potential field. The potential is $f = -0.5\,\mathrm{sech}^2\,0.1x$.

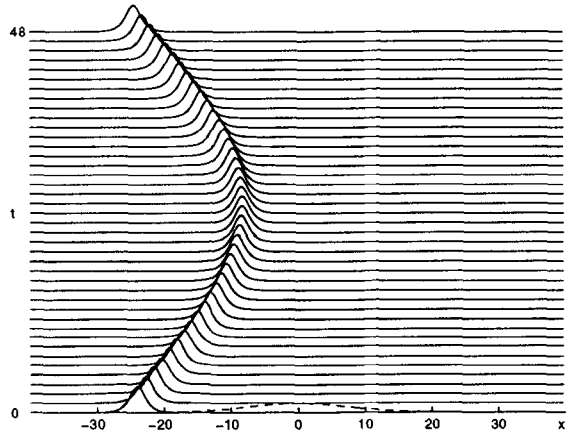

Figure 14. Reflection of a solitary wave by a potential field. The potential is $f = 0.5\,\mathrm{sech}^2\,0.1x$.

which is centered at $x_0 = -24$ and has speed 1 and amplitude $\sqrt{2}$. The solid curves are plots of $|A|$ at different times, and the dashed curve is the potential. In Figure 13, the potential $f = -0.5\,\mathrm{sech}^2\,0.1x$. As expected, we see the solitary wave passing through this potential field. In Figure 14, the potential is $f = 0.5\,\mathrm{sech}^2\,0.1x$. In this case, the solitary wave is reflected. This is no surprise because the reflection condition (4.27) is now satisfied.

The above general results can be further confirmed in the special case with $f = \alpha_0 X \equiv \alpha x$, in which case equation (4.3) is exactly solvable as shown by Chen and Liu [9]. In this case, α need not be small. With the change of variables

$$\xi = x + \alpha t^2, \qquad A = \phi(\xi, t)e^{i\alpha x t + (1/3)i\alpha^2 t^3}, \tag{4.29}$$

equation (4.3) is reduced to the nonlinear Schrödinger equation

$$i\phi_t = \phi_{\xi\xi} + \phi^2\phi^*. \tag{4.30}$$

If, initially, A is a solitary wave with speed U_0 and amplitude $\sqrt{2}r_0$, i.e.,

$$A(x, 0) = \sqrt{2}r_0 \operatorname{sech} r_0 x \; e^{-i(U_0/2)x}, \tag{4.31}$$

the exact solution at later time is

$$\begin{aligned} A(x, t) \; = \; & \sqrt{2}r_0 \operatorname{sech} r_0(x - U_0 t + \alpha t^2) \\ & e^{-i(U_0/2)x + i\alpha x t - i(r_0^2 - (U_0^2/4))t - (1/2)i\alpha U_0 t^2 + (1/3)i\alpha^2 t^3} \end{aligned} \tag{4.32}$$

Suppose $U_0 > 0$. When $\alpha < 0$, the solitary wave accelerates along the x direction and goes straightly to infinity. When $\alpha > 0$, this wave first slows down and comes to a stop at $t = U_0/2\alpha$, and then turns around and moves in the opposite direction, so that there is reflection as expected. Note the rather surprising result that there has been no amplitude change at all as the solitary wave travels through this varying potential field. When α is small, to the leading order, this exact solution is consistent with the relations (4.18) and (4.19) just derived.

Another interesting special case arises when $f = \alpha_1 X^2$. In this case, equation (4.3) is not exactly solvable, so that the perturbation results are particularly useful. When the relation (4.19) is differentiated twice with respect to T, it is found that

$$U_{TT} + 4\alpha_1 U = 0. \tag{4.33}$$

Therefore, for $\alpha_1 < 0$, the velocity U increases exponentially and the solitary wave accelerates to infinity. If $\alpha_1 > 0$, the wave is trapped and oscillates about the position $X = 0$ with the period $T_0 = \pi/\sqrt{\alpha_1}\,\epsilon$.

The knowledge gained from equation (4.3) can be used to explain the numerical interaction behaviors described earlier.

Suppose two solitary waves, with initial conditions given by (4.1) and (4.2) and well separated, come together. If a new coordinate system is chosen moving with velocity U_{B0}, the B wave is fixed relative to this system, and the A wave can be considered as moving into the varying "potential field" with $f = -\beta|B|^2$ and at initial speed $U_{A0} - U_{B0}$. Although this "potential field" is no longer slowly varying, nor is it steady, the qualitative interaction behaviors can still be understood by the results obtained for equation (4.3). For example, when $\beta > 0$, the A wave is expected to pass through, and this is confirmed in Figures 7 and 8. Its reshaping and the generation of daughter waves are due to the non-slowly varying "potential field." The same analysis applies to the B wave, and its motion is similarly understood. When $\beta < 0$, the A wave is expected to be reflected back

if $U_{A0} - U_{B0}$ is not large, as confirmed in Figure 9. In this case, the relation (4.19) for equation (4.3) gives the approximate reflection condition for the A wave as

$$\frac{(U_{A0} - U_{B0})^2}{4} < -2\beta r_{B0}^2. \tag{4.34}$$

The motion of the B wave can be analyzed similarly, and the approximate reflection condition for the B wave is

$$\frac{(U_{A0} - U_{B0})^2}{4} < -2\beta r_{A0}^2. \tag{4.35}$$

Note that as long as one of these two reflection conditions is satisfied, the two waves will be reflected. The implication is that when $\beta < 0$, the approximate reflection condition for the two initially well-separated waves (4.1) and (4.2) is

$$\frac{(U_{A0} - U_{B0})^2}{4} < -2\beta \max(r_{A0}^2, r_{B0}^2). \tag{4.36}$$

This condition is satisfied in Figure 9, and reflection is observed. The condition is not satisfied in Figure 10, and it is found that the two waves break apart with part of the energy being transmitted and part reflected.

Suppose, initially, that the two solitary waves given by (4.1) and (4.2) are completely overlapping, i.e., $x_{A0} = x_{B0}$. Analysis based on (4.18) and (4.19) shows that, when $\beta < 0$, each wave gains speed as it leaves the other. Therefore, they both escape as in Figure 12. When $\beta > 0$, each wave loses speed as it tries to leave the other. If $U_{A0} - U_{B0}$ is small, they trap each other and form a bound, oscillating state, as in Figure 11. The approximate trapping condition is given by

$$\frac{(U_{A0} - U_{B0})^2}{4} < 2\beta \min(r_{A0}^2, r_{B0}^2). \tag{4.37}$$

When β is small and positive, the two trapped waves are able to retain their initial forms without much reshaping and radiation.

5. The initial-value problem

In the previous section, solitary wave interactions for small and moderate values of the coupling coefficient β were considered. When β is large and negative, the interaction behaviors remain qualitatively the same. But when β is large and positive, the interactions reveal some new features, as shown in Figure 15. As expected, after interaction, the two solitary waves are significantly reshaped; large daughter waves are created; and radiation is also shed. A novel feature

is that new solitary waves are created. These new waves travel at speeds very different from those of the original two solitary waves.

Interactions as shown in Figure 15 for large positive β are quantitatively complicated but qualitatively simple. After interaction, the result is only a few stable permanent waves of the form (2.1) and (2.2), together with some radiation. Recall from Section 2 that when β is positive, such stable permanent waves are abundant. Now we observe that they dominate the solution after interactions. This is clear evidence as to why the permanent waves (2.1) and (2.2) and their stability are important.

In fact, interactions of the type shown in Figure 15 seem to be quite typical for coupled nonlinear Schrödinger equations (1.1) and (1.2) when β is positive. After the interaction, the solution almost always consists of a few stable permanent waves (2.1) and (2.2), together with some radiation. This is further confirmed in Figures 7 and 8. In some cases, as in Figure 11, bound, oscillatory solutions persist after the interaction. These solutions are spatially localized and temporally periodic or quasi-periodic structures, and they actually belong to a different class of special solutions of equations (1.1) and (1.2). Clearly, this class of special solutions is more difficult to determine than the permanent wave solutions (2.1) and (2.2), but it appears that they are rarely seen in the solution after interaction, which is a little comforting.

The solitary wave interaction problem is just a special kind of an initial-value problem. For a general initial-value problem of a nonlinear system, an important but difficult question is to predict the long-time solution behavior qualitatively and quantitatively. In the case of the coupled nonlinear Schrödinger equations, while quantitative predictions are difficult without the help of numerical computations, qualitative predictions seem to be relatively easy. Specifically, when β is positive, the long-time solution only consists of a few stable permanent waves (2.1) and (2.2), and in relatively rare cases, some spatially localized and temporally periodic or quasi-periodic solutions and some radiation, which is somewhat like the solitary wave interaction problem just discussed. This fact was confirmed by all our numerical calculations of equations (1.1) and (1.2) with various initial conditions.

When β is negative, it is known from Section 2 that the permanent waves (2.1) and (2.2) are always unstable unless they are degenerate, i.e., one of A and B is zero. In other words, the A and B parts tend not to stay together but to exclude each other. This has a direct impact on the long-time solution behaviors of equations (1.1) and (1.2). In fact, in both a solitary wave interaction problem and an initial-value problem, when the time becomes large, the A and B parts of the solution become separated. Inside each part, the other part is expelled. At the same time, some radiation is also shed. Two examples have been given in Figures 9 and 12. Two more examples are shown in Figures 16 and 17. In all these examples, the tendency of the A and B parts to separate is very clear. After the A and B parts are separated, each part is governed by a single nonlinear Schrödinger equation,

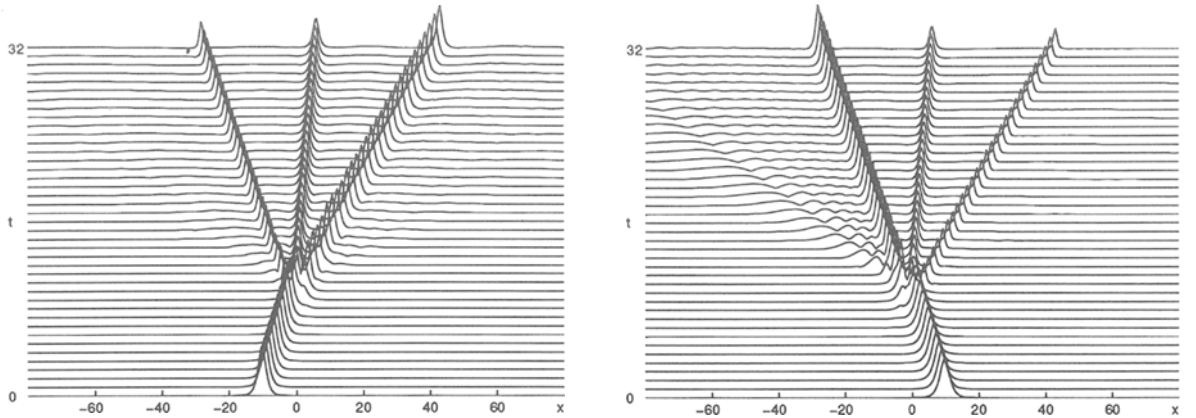

Figure 15. The interaction of two solitary waves for $\beta = 6$. The initial condition is given by (4.1) and (4.2) with $r_{A0} = 1, U_{A0} = 1, x_{A0} = -10; r_{B0} = 0.8, U_{B0} = -1, x_{B0} = 10; 0 \leq t \leq 32$. The top figure is the $|A(x, t)|$ plot, and the bottom figure is the $|B(x, t)|$ plot.

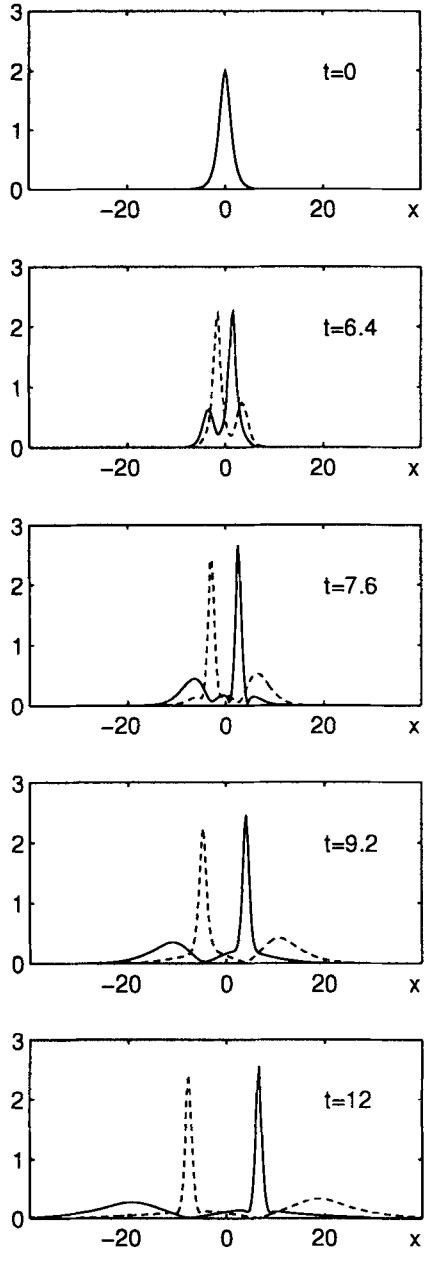

Figure 16. Instability and time evolution of the equally mixed solution (3.1) for $\beta = -0.5$. The initial condition is $A(x,0) = B(x,0) = 2\,\mathrm{sech}\,x$. Solid curves are $|A(x,t)|$ plots, and dashed curves are $|B(x,t)|$ plots.

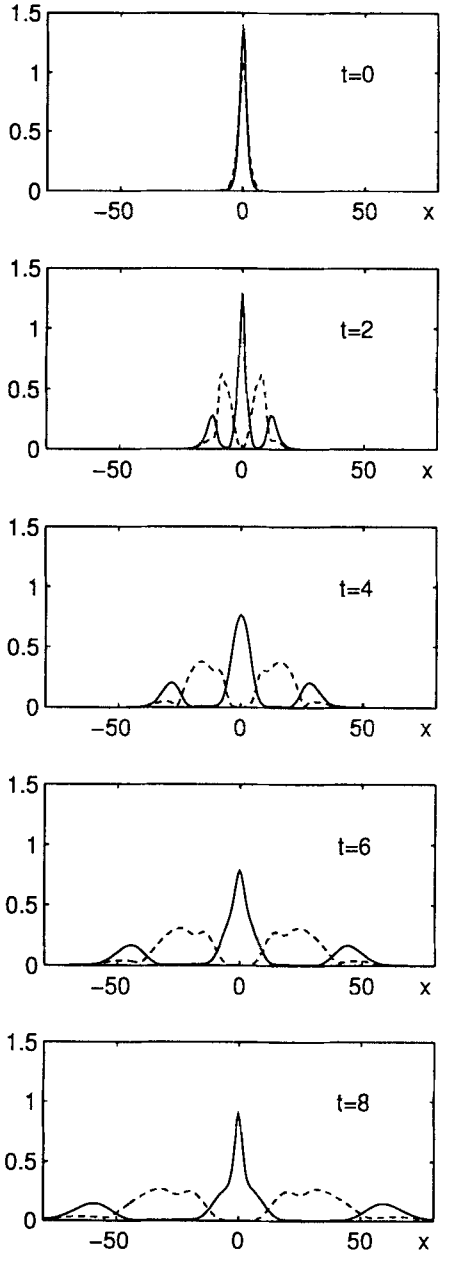

Figure 17. The initial-value problem of equations (1.1) and (1.2) for $\beta = -6$. The initial condition is $A(x,0) = 1.4\ \mathrm{sech}\ 0.9x$, $B(x,0) = 1.1\ \mathrm{sech}\ 0.7x$. Solid curves are $|A(x,t)|$ plots, and dashed curves are $|B(x,t)|$ plots.

and its later evolution can be predicted by inverse scattering theory. The final state of the solution consists of a few (stable) degenerate permanent waves such as (2.5), and, in relatively rare cases, some spatially localized and temporally periodic solutions together with some radiation.

6. Conclusion and speculation

In this paper, the coupled nonlinear Schrödinger equations (1.1) and (1.2) have been investigated. Firstly, the permanent wave solutions (of the form (2.1) and (2.2)) and their stability were determined both analytically and numerically. It was found that when $\beta > 0$, stable permanent waves are abundant; but when $\beta < 0$, only degenerate permanent waves are stable. Secondly, solitary wave interactions were explored numerically, and various interaction behaviors have been explained analytically. Finally, the long-time solution behavior with general initial conditions was investigated. It was found that the stable permanent waves almost always dominate the long-time behavior of the solution.

It is not unreasonable to expect that some of the results obtained for these coupled nonlinear Schrödinger equations are actually quite general and apply to many other nonlinear systems. If stable permanent waves of appropriate form are abundant in a nonlinear system, these waves are likely to dominate the long-time behavior of the solution. These permanent waves are generally solitary waves and not solitons, but nonetheless, they play a very important role in the understanding of the final state of the nonlinear system.

References

1. D. J. BENNEY and A. C. NEWELL, *J. Math. Phys.* 46:133–139 (1967).
2. G. J. ROSKES, *Stud. Appl. Math.* 55:231–238 (1976).
3. G. P. AGRAWAL, *Nonlinear Fiber Optics*, Academic Press, 1989.
4. C. R. MENYUK, *J. Opt. Soc. Am. B* 5:392–402 (1988).
5. S. V. MANAKOV, *Sov. Phys. JETP* 38:248–253 (1974).
6. T. B. BENJAMIN and J. E. FEIR, *J. Fluid Mech.* 27:417–430 (1967).
7. L. D. LANDAU and E. M. LIFSHITZ, *Quantum Mechanics: Non-relativistic Theory*, Pergamon Press 1977.
8. V. E. ZAKHAROV and A. B. SHABAT, *Sov. Phys. JETP* 34:62–69 (1972).
9. H. H. CHEN and C. S. LIU, *Phys. Rev. Lett.* 37:693–697 (1976).
10. V. V. AFANASYEV, Y. S. KIVSHAR, V. V. KONOTOP, and V. N. SERKIN, *Opt. Lett.* 14:805–807 (1989).
11. D. J. KAUP and B. A. MALOMED, *Phys. Rev.* A 48:599–604 (1993).
12. D. J. KAUP and A. C. NEWELL, *Proc. R. Soc. London* A 361:413–446 (1978).
13. Y. KODAMA and M. J. ABLOWITZ, *Stud. Appl. Math.* 64:225–245 (1981).

14. T. UEDA and W. L. KATH, *Phys. Rev.* A 42:563–571 (1990).
15. E. M. WRIGHT, G. I. STEGEMAN, and S. WABNITZ, *Phys. Rev.* A 40:4455–4466 (1989).

THE UNIVERSITY OF VERMONT
MASSACHUSETTS INSTITUTE OF TECHNOLOGY

(Received August 8, 1994)